Research Paper

Hazardous elements and amorphous nanoparticles in historical estuary coal mining area

Check for updates

Ana L. Duarte [a], Kátia DaBoit [a], Marcos L.S. Oliveira [b], Elba C. Teixeira [c], Ismael L. Schneider [a], Luis F.O. Silva [a],*

[a] Department of Civil and Environmental, Universidad de la Costa, Calle 58 #55-66, 080002, Barranquilla, Atlántico, Colombia
[b] Faculdade Meridional IMED, Passo Fundo, Brazil
[c] FEPAM-Fundação Estadual de Proteção Ambiental Henrique Luis Roessler, Porto Alegre, RS, Brazil

ABSTRACT

In Brazil, intense coal exploitation activities have led to environmental deterioration, including soil mortification, water contamination, loss of ecosystem, and atmospheric contamination. In addition, considerable quantities of sulfur-rich residues are left behind in the mining area; these residues pose grave environmental issues as they undergo sulfide oxidation reactions. When sulfur oxides come in contact with water, extreme acid leachate is produced with great proportions of sulfate, and hazardous elements (HEs), which are identified as coal drainage (CMD). CMD is an environmental pollution challenge, particularly in countries with historic or active coal mines. To prevent CMD formation or its migration, the source must be controlled; however, this may not be feasible at many locations. In such scenarios, the mine water should be collected, treated, and discharged. In this study, data from 2005 to 2010 was gathered on the geochemistry of 11 CMD discharges from ten different mines. There are several concerns and questions on the formation of nanominerals in mine acid drainage and on their reactions and interfaces. The detailed mineralogical and geochemical data presented in this paper were derived from previous studies on the coal mine areas in Brazil. Oxyhydroxides, sulfates, and nanoparticles in these areas possibly go through structural transformations depending on their size and formation conditions. The geochemistry of Fe-precipitates (such as jarosite, goethite, and hematite) existent in the CMD-generating coal areas and those that could be considered as a potential source of hazardous elements (HEs) (e.g., Cr) were also studied because these precipitates are relatively stable in extremely low pH conditions. To simplify and improve poorly ordered iron, strontium, and aluminum phase characterization, field emission scanning electron microscopy (FE-SEM), high-resolution transmission electron microscopy (HR-TEM), micro-Raman spectroscopy, and X-ray diffraction (XRD) and sequential extraction (SE) studies were executed on a set CMD samples from the Brazilian mines. This study aimed to investigate the role of both nanomineral and amorphous phase distribution throughout the reactive coal cleaning rejects profile and HEs removal from the water mine to provide holistic insights on the ecological risks posed by HEs, nanominerals, amorphous phases, and to assess sediments in complex environments such as estuaries.

© 2018, China University of Geosciences (Beijing) and Peking University. Production and hosting by Elsevier B.V. This is an open access article under the CC BY-NC-ND license (http://creativecommons.org/licenses/by-nc-nd/4.0/).

1. Introduction

Human economical activities such as coal exploitation, which is one the most ancient and essential human activity associated with human development, adversely impact the environment, indebting us to mother nature (Pruvot et al., 2006; Aleksander-Kwaterczak and Helios-Rybicka, 2009; Silva et al., 2009a, b). Historically, the coal mining activities in Brazil used to be carried out without effective environmental regulations and controls. The activities were performed disregarding environmental issues, concomitantly leading to diffuse contamination. One of major concern in Brazil is to continuous control and monitor requirements of abandoned or inactive coal mines. In these areas, tailings containing coal cleaning

residues (CCR) and pore ore with very high contents of hazardous elements (HEs) are being accumulated at a large speed; these compounds usually lead to the formation of acidic, metal-rich aquatic effluents (Silva and Wollenschlager, 2010a, b).

In addition, another concern in coal areas is related to coal mine drainage (CMD) sediments since they can act as both a source and a sink for contaminants. CMD is an important phase for controlling metal toxicity in organisms (Galatto et al., 2009). There are over 1000 abandoned mines in Santa Catarina, south Brazil (Lattuada et al., 2009). The efficiency of H_2O treatment plants of some active coal mines is low for such types of contaminants. In this region, some of the rivers are considered dead, apart from CMD (Silva and Wollenschlager, 2010a), they receive domestic effluent and agricultural discharges that further increase the toxicity levels and seriously impact aquatic ecosystems (Marcello et al., 2008; Galatto et al., 2009). Since Brazilian coal mining activities cause serious disturbances in the trophic chains and the ecosystem, and considering that this pollution is occurring over the last 50 years, it is hypothesized that the ecological circumstances have occasioned in a destruction event, which might have formed predominantly toxic CMD geochemistry that is heartwarming the communities. Brazilian coal mine effluents are typically acidic in nature due to sulfur oxidation (in special Fe-sulfides) (Silva and Wollenschlager, 2010a). Extremely low pH increases the dissolution speed of toxic elements (e.g., As, Hg, Se, and Cd), enabling their transport in leachates from CCR (Silva et al., 2010b).

Coal cleaning residues are composed of variable quantities (generally 1%–10%) of "pyritic-sulfur" (including other iron sulfide minerals such as marcasite) and organic sulfur (Silva et al., 2010c). These contaminants form complexes with organic materials and get sedimented in effluents, leading to an acidic pH shift in the effluent. This may remobilize them into pore water and subsequently into the overlying water column (Antunes et al., 2007). Anthropogenic activities impact estuarine waters and/or riverine inputs via HEs contamination, which may be environmentally relevant in the case of tropical estuaries (Balachandran et al., 2005). Superficial sediments with diverse particle size may be resuspended in the air due to tropical storms and may also be dispersed and accumulated across different sedimentary environments (Guillén et al., 2006). Furthermore, storms increase water volumes coming from leachates on surrounding mine soils (Zimmer and Lautz, 2014). The absorptive nature of hazardous elements facilitates their accumulation on fine-grained sediments, subsequently acting as an important reservoir of contaminants that have a high probability of mobilization (Eggleton and Thomas, 2004; Schneider et al., 2014). The bioavailability and toxicity of HE ions in aquatic ecosystems may be impacted by their solubility in the sediments; this solubility increases with the increasing total concentration of HEs in the estuarine water (Silva et al., 2010d). Sediments are fundamental for the community's equilibrium as they constitute a reservoir of organic and inorganic material essential for many vital cycles (Wong et al., 1999). However, when the equilibrium is disturbed, sediments also act as pollutants in the ecosystems, a feature that is intimately connected with the contaminant's bioavailability (Burton, 2002; Schneider et al., 2014). This parameter depends on the physical and chemical characteristics of pore water (e.g., pH, hardness, and redox potential) since they determine the solubility of chemical substances in the water (Admiraal et al., 1995; Vaufleury and Pihan, 2002).

Potential synergistic and antagonistic relationships between contaminants and the level of organic compounds on sediments (Allen et al., 1995) may complicate interactions between contaminants and sediments. The techniques such as Mössbauer spectroscopy (Silva and Wollenschlager, 2010a), visible near-infrared reflectance (vNIR) (Alpers et al., 2008; Bishop et al., 2008), micro-

Raman spectroscopy (M-RS) (Silva and Wollenschlager, 2010a, b, c, d), synchrotron X-ray diffraction (XRD), X-ray fluorescence (XRF) (Root et al., 2007), X-ray absorption near-edge structure (XANES) (Alpers et al., 2008; Bishop et al., 2008), and extended X-ray absorption fine structure (EXAFS) (Alpers et al., 2008; Chen and Jiang, 2008) have been recently used to analyze rich and reasonably crystallized phases related to some metal adsorption and coprecipitation processes, which, along with pH buffering, also contribute to complex mineralogical control that both phases have on CMD hydrogeochemistry.

The Tubarão estuary is affected regularly by strong storms, which could change or affect the biogeochemistry of the area; however, environmental effects of these events on a polluted aquatic system are not usually studied (Birch and Taylor, 1999). Therefore, this study aimed at the following:

(1) determining the mineralogical and assemblage characteristics of CMD from Brazilian coal mines including stream waters impacted by acid mine drainage (AMD); this objective may help understand sediment quality from CMD at Santa Catarina, south Brazil, by sequential extraction procedures;
(2) assessing the pollution of HEs in stream sediments;
(3) comparing the data with metal concentrations at bottom sediments from similar historical mines and smelting areas in Brazil and other countries;
(4) building an initial database focused on the current status that enables recovery plans for areas affected by coal mining activities. Because of the presence of very complex mixtures of minerals and contaminants (especially HEs) in sediments of Brazilian coal mining areas and the potential for toxicological interactions among them, effects-based testing has been used to evaluate sediment toxicity;
(5) estimating storm events significance on HEs mobility from polluted sediment in a tropical estuary.

2. Methods

2.1. Sampling and preparation

The environmental coordinates (latitude/longitude) of the CMD sampling areas were recorded by Etrex® GPS and then plotted on an area map. CMD was photographed (Fig. 1), and its extension was measured when possible (Table 1). All plastic and glass materials were washed with soap and water, rinsed with Ellix quality water (κ < 0.2 μS/cm, Millipore), and kept in a 10% nitric acid (Panreac) bath for 24 h. Furthermore, all the materials were thoroughly rinsed with Ellix and MilliQ water (κ < 0.05 μS/cm, Millipore) before use. Syringes rinsed with acid water using the manual suction kit were used to store the ochreous, colloidal precipitates, whereas solid samples were directly stored in polyethylene bottles. At the collection site, the samples were stored in closed plastic bags and transported to the laboratory to prevent mineralogical changes. Sediment samples were chemically analyzed using the method described by Rodriguez-Iruretagoiena et al. (2016). CMD sampling protocol is a statistically-based, cost-effective method not only to screen and prioritize mine waste piles for remediation on a regional or a watershed scale but also to construct an extensive and diversified database that could assist CMD modeling efforts on Brazilian mining sites. Sampling error and sample size were reduced using a <2 mm fraction, which also provided a worst-case scenario estimation for metal leachability (Hammarstrom et al., 2003, 2005). All sediments were sampled using a plastic shovel and gloves and deposited in sealed plastic container. Once in the designated laboratory, sediments samples were controlled dried at 40 °C for 24 h.
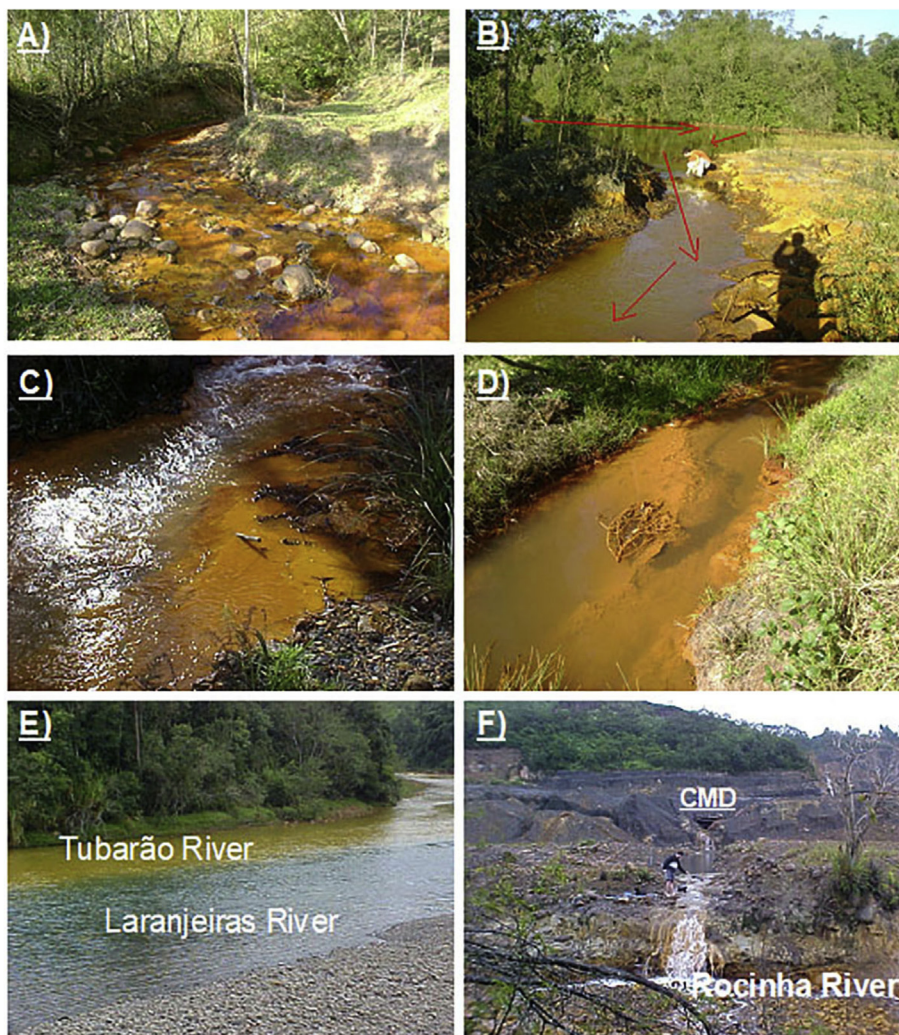
Figure 1. The typical CMD and impacted rivers from Santa Catarina area, Brazil. (A) Rastro (DR 4); (B) Lingua do Dragão (Treviso city − DR 3); (C) Urussanga (Urrusanga City − DR 6); (D) Banhado da Estiva (Capivari de Baixo city − DR 10); (E) Tubarão/Laranjeiras Rivers (GPS S 2821591, W 4918873); (F) Rocinha River (Lauro Müller city, GPS S 2823691, W 4923890).

Inductively coupled plasma mass spectrometry (ICP-MS), inductively coupled plasma atomic-emission spectrometry (ICP-AES), XDR, Raman, field emission scanning electron microscopy (FE-SEM), and high-resolution transmission electron microscopy (HR-TEM) were used to analyze the multi-element geochemical compositions of air dried split samples (Silva et al., 2009b). Organic dissolvent suspensions were selected to prevent mineralogical transformation in separate solvents and to disperse inorganic powders, a commonly used technique for HR-TEM (Chen et al., 2004; Silva et al., 2009b, 2010b) and FE-SEM sample preparation. The sample material can be easily dissolved in the suspension as the suspension medium can break up aggregations, enabling physical separation of individual particles for electron microscope analysis. The suspension was placed on lacy carbon films supported by copper grids HR-TEM/STEM/EDS. Although this technique may lead to agglomeration, it is a widely used standard procedure for most minerals, including metal sulfates (Giere et al., 2006). To minimize contamination previously SEM and scanning transmission electron microscopy (STEM) analysis, a modern plasma method (Gatan Model 950) was used to clean the specimen holder.

The geochemical analysis of CMD sediment subsamples was performed with different procedures of sequential extraction (SE). The five essential factors that define an SE procedure are as follows:

(1) geochemical factors, employed for the different extractants (such as water, $C_2H_8N_2O_4$ with different concentrations); (2) solid-extractant volume ratio ($<$0.177 mm); (3) species and nature of the interaction among the solid sediment, extractant, and environmental circumstances during each step of the sequential extraction; (4) time; and (5) replicate extraction number. Details explaining SE conditions are demonstrated:

(1) Water mobile portion: 9 mg of the CMD sediment (tree replicates) were mixed with 0.1−0.5 μS/cm electric conductivity Millipore water system. Subsequently, the samples were shaken for 4 h, centrifuged (3000 rpm for 10 min) and finally filtered ($<$22 μm) in a dark room. Continuous pH measurements allowed natural acid production potential. The extraction solvent dissolves gypsum, jarosite, alunogen, chalcanthite, hexahydrite, copiapite, epsomite, ferrohexahydrite, melanterite, rozenite, zugshunstite (Ce) and others minerals soluble in water. The initial water extraction step and secondary sulfates and salts in CMD environments are vital for completely understanding the environments

(2) Poorly ordered Fe^{3+} oxyhydroxides/sulfates: 9 mg of the CMD sediment (tree replicates) was mixed with water and ammonium oxalate reagent (28 g/L ammonium oxalate + 15 g/L

oxalic acid solution; pH of approximately 2.7) and then shaken in the dark for 4 h (Gagliano et al., 2004; Regensburg et al., 2004). The samples were then centrifuged (3000 rpm for 10 min) and filtered (<22 μm) (Peretyazhko et al., 2009). Poorly crystalline Fe(III) oxides (ferrihydrite and schwertmannite) dissolved in the preparation due to the presence of more insoluble crystalline Fe(III) oxides (e.g., goethite and hematite) (Cornell and Schwertmann, 2003); $>85\%$ of the total iron is released during this step.

(3) Very ordered Fe(III) minerals: ammonium acid oxalate (Kumpulainen et al., 2007) partially dissolves sulfate-rich CMD crystalline iron precipitates (hematite and goethite) during an sequential extraction step, as reported by Dold (2003a, b). However, in the method proposed by Dold, 0.2 M NH₄ oxalate was used as the extractant for 2 h in step 2, but in this study, the samples in batch system were exposed to light and heated to 80 °C in a water bath.

3. Analytical techniques

3.1. Mineralogical methods

Solid samples were mineralogically characterized using a D5005 XRD Siemens powder model with a monochromator diffracted beam. Scans with 0.5 s counting time per step and $0–60°$ 2θ were used on sediment and sulfate salt samples for routine XRD inspections. The Renishaw model via the Reflex Raman coordination was controlled in the confocal mode (approximately 1 μm, Guedes et al., 2008). Extended scans were performed on each sample. Thermal decomposition was prevented using a density filter on the Raman sample spectra measurement. Advanced electron bean equipments were performed with previously reported by ours previously published works (Tiede et al., 2009; Silva and Wollenschlager, 2010a, b).

3.2. Chemical methods

An elemental analyzer (vario MACRO) was utilized to determine the concentration of carbon, sulphur, hydrogen, and nitrogen in the studied sediment samples. Hg analysis was performed by a LECO AMA 254 equipment.

ICP-MS (X series II), in a pulse counting mode (three points per peak), was applied to research HEs. The ICP-MS analysis and sediment sample microwave digestion program were outlined by Dai et al. (2011a, b). Se and arsenic were determined using collision cell technology.

Si analysis were performed by X-ray fluorescence spectrometry (XRF, ARL ADVANT'XP+), as outlined by Dai et al. (2011a,b). The sediment samples were prepared by borate fusion in an automated fusion furnace.

Table 1
Studied CMD area localization.

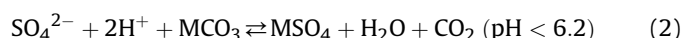|	Drainages	City
DR1	Carbonífera Caratarinese	Lauro Muller
DR2	Carbonífera Caratarinese	Lauro Muller
DR3	Língua do Dragão	Treviso
DR4	Rio do Rastro	Lauro Muller
DR5	Carb. Siderópolis	Urussanga
DR6	Mina Abandonada Urussanga	Urussanga
DR7	Mina São Geraldo	Criciúma
DR8	Carbonífera COMIN	Criciúma
DR9	Banhado da Estiva/córrego esquerdo	Capivari de Baixo
DR10	Banhado da Estiva/córrego direito	Capivari de Baixo
DR11	Banhado da Estiva/corrego seco	Capivari de Baixo

4. Results

4.1. Sediments mineralogy

CMD mineralogy is quite diverse (Table 2). At Santa Catarina, the Fe^{3+} phases in coal discharges have been researched in detail. Traditionally, they were known as "efflorescence" (e.g., melanterite, rozenite, and alunogen), "ochreous precipitates" (e.g., jarosite, schwertmannite, and goethite), "crust from cementing processes" (e.g., kaolinite, illite and iron phosphate), "amorphous iron oxides," "ferric hydroxides," or "poorly crystalline oxyhydroxides" (Table 2). The CDM usually found in Santa Catarina (Table 2 and Fig. 1) has been previously characterized mineralogical and chemical properties. The evolutionary process can be understood owing to the presence of melanterite, jarosite, and Ca-sulfates, which are typically agglomerated in the encrustation environment (Valente and Gomes, 2009). Therefore, our efforts were focused on characterizing these mineral. The rivers affected by CMD (Fig. 1) have yellow to reddish brown sediments on their banks; these abundant "ochre precipitates" consist of iron minerals and amorphous constituents mobilized in CMD coming from Fe-sulfides (Fig. 2A) and sphalerite (Fig. 2B) oxidation in the CMD. We believe that this is the most generalized feature of the present zone. After ore processing, arsenic rejects are typically stored within abandoned tailings. The subsequent reaction and leaching of arsenic is an additional health hazard.

Zinc sulphide oxidation and dissolution rates intensification with the increasing iron concentration in the mineral (Fig. 2C; Blowes et al., 2003). In the lab observations, low iron and high iron sphalerites present a fast primary leaching, releasing zinc from the mineral external, following which, the reaction rate intensely slows down (Buckley et al., 1989; Stanton et al., 2008). These sediments with a ultrafine/nano-grain size and highly crystalline nature offer a challenge in the geochemistry characterization step compared with other well crystallized minerals of Fe-sulfide oxidation such as Fe-hydroxide (Fig. 3A), Fe-oxide (Fig. 3B), or Fe-sulfate (Figs. 4–6). Sulfate minerals are known for their preservative properties for both chemicals and morphological fossils (Bonny and Jones, 2003); therefore, it is important to understand their role in metal cycling, especially in CMD environments and sulfate deposits. Well preserved fossils in the iron precipitates of the Brazilian coal mines include minute fossils of coccid and microorganisms (Fig. 6). Ca, Fe, Ba, Mg, Cu, K, and Na sulfates were identified in the Brazilian samples (Table 2). These sulfates may be epigenetic or may be weathering products of other minerals. The following reaction may occur from primary Fe sulfide minerals oxidation (Silva and Wollenschlager, 2010a, d) to secondary sulfate minerals if the metal carbonates are available to soluble sulfate ions, releasing bicarbonate ions at the current pH of natural waters:

$$SO_4{}^{2-} + H^+ + MCO_3 \rightleftarrows MSO_4 + HCO_3 \ (pH > 7.2) \qquad (1)$$
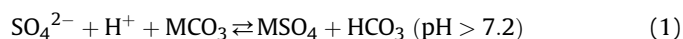
or CO_2 in acidic water scenarios:

$$SO_4{}^{2-} + 2H^+ + MCO_3 \rightleftarrows MSO_4 + H_2O + CO_2 \ (pH < 6.2) \qquad (2)$$

Chemical species such as alkali and alkaline earth HEs, transition HEs and aluminum are possibly produced during reactions. Among the calcium precipitates, mainly as gypsum and calcite, gypsum (Fig. 4) is very abundant in wet conditions and in most CMD under all weather conditions. In our investigation, gypsum was easily identified after water extraction. In general Ca-hydrated sulfate is slightly soluble in acid water, but much less leachable than any of the other sulfate observed at the study areas. There was clear

Table 2
The mineral composition of the CMD at Santa Catarina.

	DR1	DR2	DR3	DR4	DR5	DR6	DR7	DR8	DR9	DR10	DR11
Silicates											
Quartz, SiO_2	a–d	a,c,d	b–d	a–d	a,d	a–d	a–d	a,d	a,c,d	b,d	a,c,d
Clay Minerals:											
Kaolilite, $Al_2Si_2O_5(OH)_4$	a,c,d	a–d	c,d	a,d	a,c,d		a,d	a,d	d	a,d	
Illite, $K_{1.5}Al_4(Si_{6.5}Al_{1.5})O_{20}(OH)_4$											
Chlorite				d					d		
$Na_{0.5}Al_6(Si,Al)_8O_{20}(OH)_{10} \cdot H_2O$											
Interstratified Clay minerals:				b		d					
K feldspar, $KAlSi_3O_8$											
Albite, $NaAlSiO_8$				a,d							
Metakaolin, $Al_2O_3 \cdot 2SiO_2$						b–c			a–d		
Microcline, $KAlSi_3O_8$				a,d		b–d					
Mullite, $Al_6Si_2O_{13}$							b				
Melilite, $CaAl_{12}MgSi_3O_{14}$								b	c		
Plagioclase, $(Na,Ca)(Al,Si)AlSi_2O_8$									b		
Zircon, $ZrSiO_4$	d				b				d		
Suphides											
Pyrite, FeS_2		b–c				b–d	b,c				
Marcasite, FeS_2									b		
Pyrrhotite $Fe_{(1-x)}S$						b					
Galena, PbS				c		b–c					
Sphalerite, ZnS		b–d				b–d	d				d
Carbonates											
Calcite, $CaCO_3$			d								
Aragonite, $CaCO_3$					d			c			
Dolomite, $CaMg(CO_3)_2$	b				d						
Sulphates											
Gypsum, $CaSO_4 \cdot 2H_2O$	b,d	d			b–d	b,c	b–d	b–d	d	a–d	a–d
Barite, $BaSO_4$			c			c			d		
Natrojarosite, $NaFe_3(SO_4)_2(OH)_6$	b–d			d						b	d
Jarosite, $KFe^{3+}{}_3(SO_4)_2(OH)_6$	a–d	c,d			a–d	b	d	a,c,d	a–c	d	d
Hexahydrite, $MgSO_4 \cdot 6H_2O$	a,b–d				b–d	b–c	d	c	c–d	d	
Calcantite, $CuSO_4 \cdot 5H_2O$	a,c,d	d			b,c			d	b	d	c–d
Schwertmannite, $Fe^{3+}{}_{16}O_{16}(OH)_{12}(SO_4)_2$	d		b–d	d		d	b,d	d	b–c		d
Alunogen, $Al_2(SO_4)_3 \cdot 17H_2O$			b–d		b,d	b,d	d	c,d	b–d	b	
Copiapite, $Fe^{2+}Fe^{3+}(SO_4)_6(OH)_2 \cdot 20H_2O$	d				d		d		d		b,d
Epsomite, $MgSO_4 \cdot 7H_2O$					c–d				c		d
Ferrohexahydrite, $FeSO_4 \cdot 6H_2O$	c					d			d		
Melanterite, $FeSO_4 \cdot 7H_2O$						d			d		
Rozenite, $FeSO_4 \cdot 4H_2O$						d			d		
Oxides and hydroxides											
Hematite, Fe_2O_3									b,d		
Goethite, $Fe(OH)_3$	b–d								a–d		
Gibbsite, $Al(OH)_3$	a,c,b	b,d	d	a,b,d	a–d		b		b	a,b	
Brucite, $Mg(OH)_3$					d	b,d	c,d	d	d		

[a] XDR.
[b] FE–SEM.
[c] HR–TEM.
[d] Raman.

indication of mineral or amorphous aluminum phase by EDS (Figs. 4 and 5), but not with XRD. Large aluminum quantities in CMD sediments indicate that amorphous must be current. Minerals, such as basaluminite, help understand the behavior of Al acid solutions and they control the aluminum occurrence at the low pH (España et al., 2005). Al-phases with gibbsite for example is usually unstable at a pH of <5.5 (depending on sulfate activity); however, it is rarely found in acid-sulfate environments (Silva and
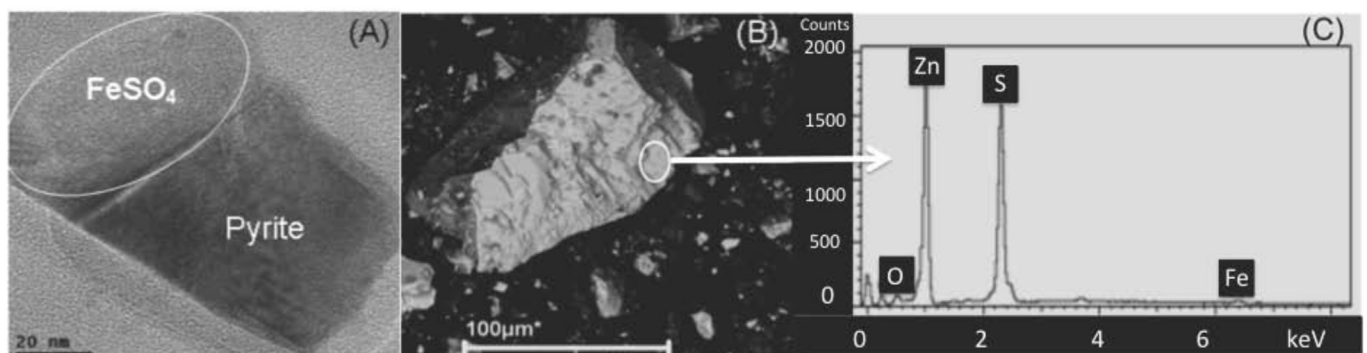

Figure 2. (A) The example of nanopyrite (TEM image after SE) in sediments of CMD (DR 7) after selective extraction/complexation with ammonium oxalate and water; (B) An SEM image of sphalerite in sediments from DR6 and EDS.
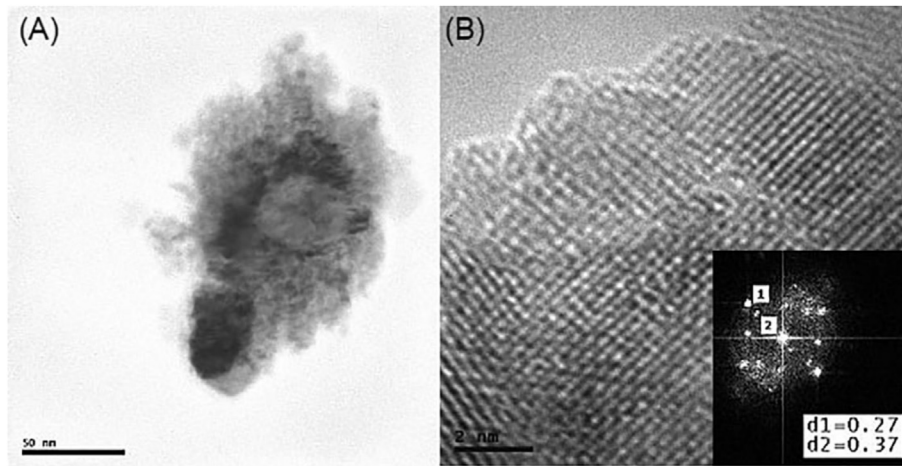
Figure 3. Nanominerals in CMD. (A) Goethite present on cementation by fine-grained material (TEM image after SE); (B) Nanohematite (HR-TEM image after SE) from CMD (DR1) with fast Fourier transformation (FFT) to confirm the structure.

Wollenschlager, 2010a). Others rare minerals with for example jurbanite precipitation take place at a pH of <4; this compound is the most stable mineral CMD sediment (España et al., 2005). The CMD-contaminated sediment samples contained amorphous Al oxyhydroxysulfate (probably basaluminite) at a pH of >4 and a geochemical accumulation of Fe-sulfate-hydroxides in CMD at a pH of 2—4. The presence of aluminumsilicates as gangue and wall rock minerals was confirmed at all the work areas; the Fe—Al-salt

geochemistry reflect the composition of the detected phases deposits (Table 2). Calcite is mostly found inside consolidated crusts, but it was rarely converted in macroscopic samples at waste dumps.

4.1.1. Iron precipitates

In the ecosystem, iron is not easily available as it reacts with oxygen to form oxyhydroxides, making it a major limiting nutrient. However, there are places where iron abundance is visibly high due
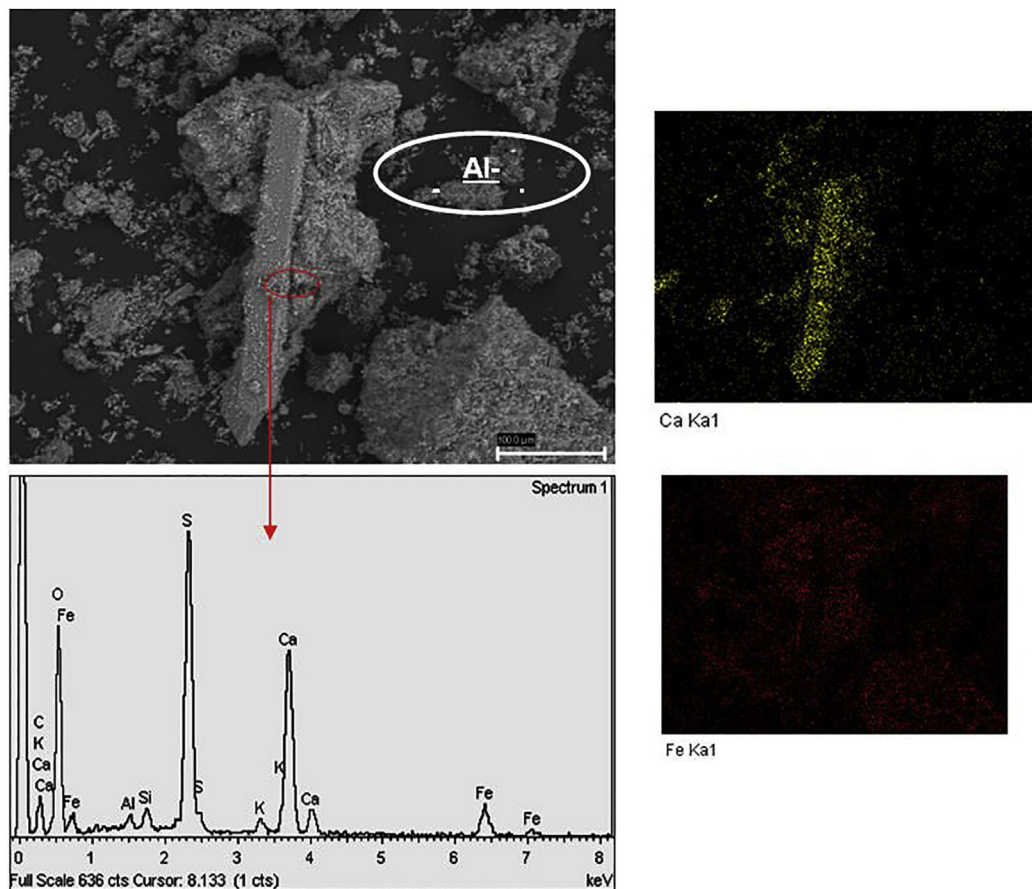

Figure 4. Jarosite is also accompanied by gypsum and Al-amorphous faces in sediments from CMD (SEM image-DR10 after SE).
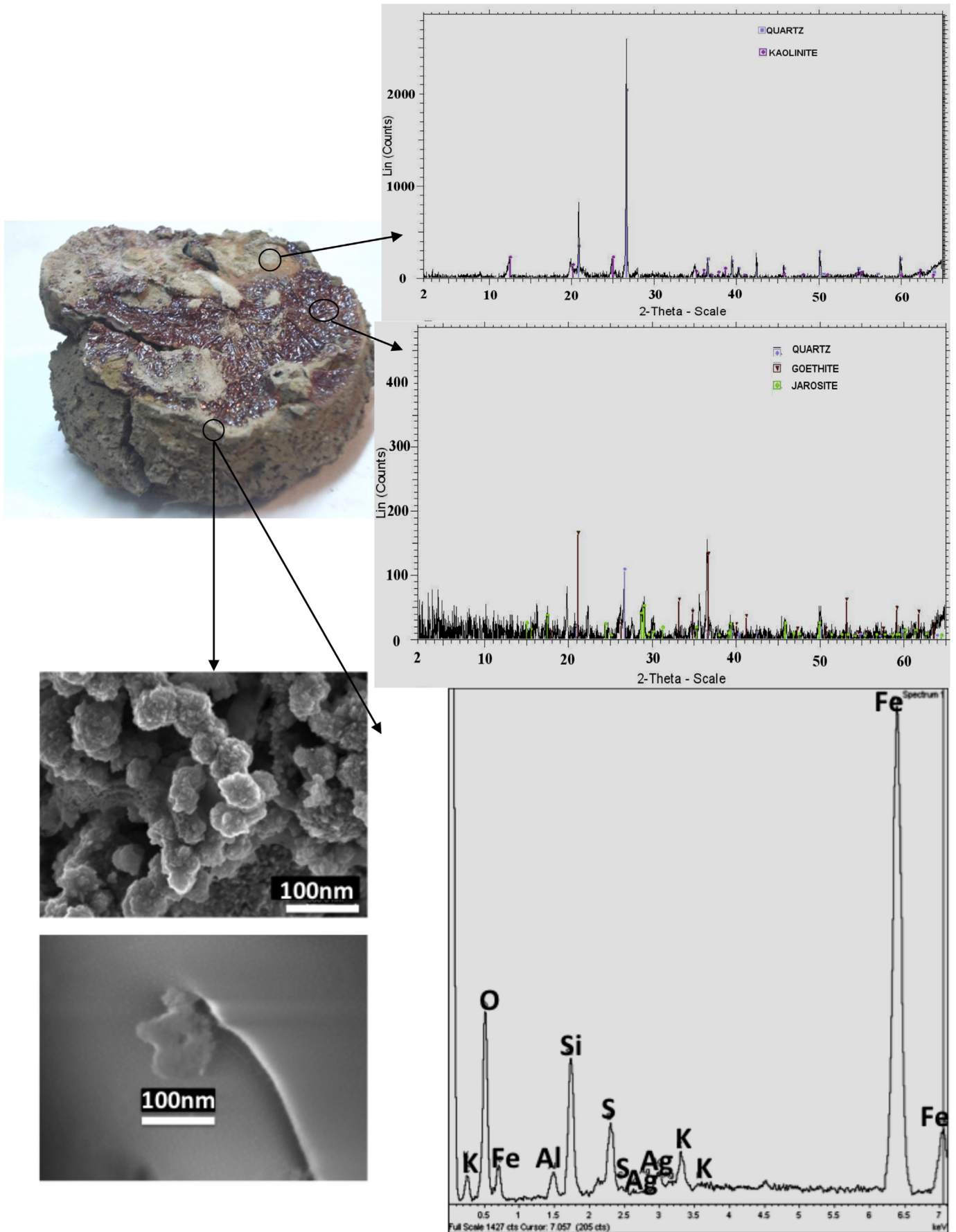
Figure 5. The selective extraction of CMD sediments with acid ammonium oxalate to obtain clean jarosite crystals.
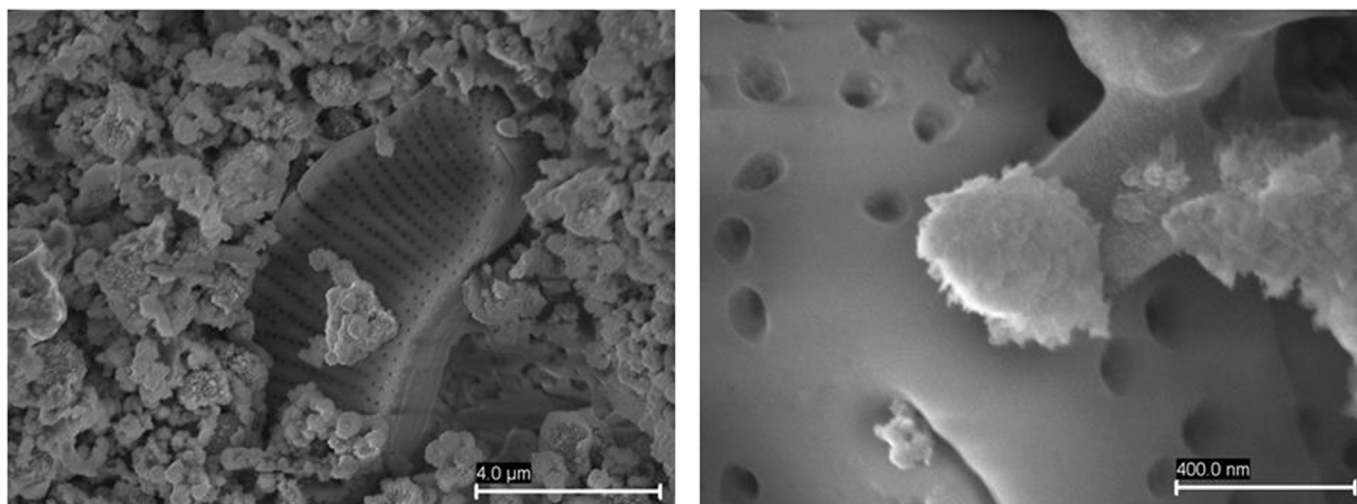
Figure 6. Preserved minute fossil on DR1 (cementing by jarosite).

to the rusty color owing to the large amount of ferric hydroxides CMD (Fig. 2). Iron is a major element found in the acid coal drainage samples.

The iron sulfates list contains mainly modest Fe-salts. For example, rozenite and melanterite were usual CMD water soluble Fe phases appearing as efflorescence. Fe^{3+} was originating in moderately insoluble hydroxides and hydroxysulfates. The analyzed minerals on CMD samples are linked to metal absorption due to the larger iron precipitate-specific surface area, confirming that arsenic, chromium, lead, cadmium, and zinc occurrence of samples ranged between tens to a few thousand part per million (Table 4). Detected concentrations were higher than those detected for the sediments samples dominated by SiO_2 and Al–Si–O phases (Table 2). In this case, iron may represent a hazardous risk to life due to its relations with As, Cd, Cu, Hg, Pb, Zn, and other elements that may be leached out from CCR (Silva et al., 2010b). The results are aligned with the data available on HE sorption on hydrous Fe^{3+} oxide in CMD (Silva and Wollenschlager, 2010a), demonstrating that HE preservation by sorption onto iron and aluminum ultra-fine/nanometric precipitates can be real mechanisms for normal attenuation of leach HEs (Fukushi et al., 2003). Additionally, growth kinetics may be altered due to Fe oxyhydroxide nanoparticle (e.g., goethite presented by Fig. 4A) structural transformations, depending on their size and formation conditions displaying a crystallographically oriented form of aggregation at nanoscale

(Waychunas, 2009). Hematite surface nonstoichiometry (Fig. 3B) suggested that at least one Fe oxyhydroxide may be stable on a nanoscale and it is also possible that the geochemistry of other natural oxides may be size dependent. Detected ochre precipitate impurities include several Fe-minerals such jarosite, schwertmannite, and goethite as main components when present in CMD. The most iron-rich hardpans cement compositions include the ferrihydrite and lepidocrocite, which have restricted occurrences internal solid masses associated with additional minerals such as sulfur and goethite. The main compound of CMD (Figs. 4 and 6) is 5 nm to 1 μm jarosite that forms euhedral, pseudocubic crystals. Utilized procedure by $C_2H_8N_2O_4$ and water extraction held in the nonexistence of light resulted in the formation of relatively pure jarosite and goethite on the subsamples (see Fig. 5) of the shallow acidic CMDs along stream channels. Table 2 shows the TEM and SEM analysis that detects Fe hydroxysulfates mixtures with the general formula $MFe(SO_4)_2(OH)_6$ (M = NH_4^+, H_3O, Na, K, Rb, and ½Pb); these mixtures that belong to the jarosite group of minerals (Nielsen et al., 2008). Investigates CMD analysis using FE-SEM indicated that jarosite formed in several drainages was associated in large aggregates; they occur in nature, where they are generally formed in the acidic aqueous environments and are often related and linked to CMD, especially in CMD sites. Jarosite bulk samples in EDS analysis group of minerals showed that there are no significant sinks for toxic ions such as arsenate, chromate, thallium, lead, and

Table 3
The measured parameters of CMD waters and the main elements (%) in contaminated sediments.

	DR1	DR2	DR3	DR4	DR5	DR6	DR7	DR8	DR9	DR10	DR11
pH	2.49	3.88	3.06	2.37	3.66	2.68	2.91	3.89	3.42	2.98	2.56
Eh (mV)	478	302	427	462	346	401	419	384	344	385	459
SO_4^{2-} (g/L)	4.97	0.98	2.04	3.29	1.26	2.01	1.98	1.44	1.54	3.05	4.59
Temperature (°C)	21.3	19.7	20.6	20.4	20.4	21.2	21.6	20.3	18.6	19.4	21.7
EC (mS/cm)	2.64	1.39	2.03	2.42	2.38	2.40	2.18	2.16	2.01	1.98	2.39
Al	0.42	1.72	3.62	1.64	8.82	8.82	6.76	8.43	5.50	6.67	2.12
Ca	0.05	0.01	⟨0.01	0.09	0.19	0.05	0.04	0.09	0.07	0.14	0.32
Cr	<0.01	⟨0.01	<0.01	<0.01	<0.01	<0.01	<0.01	<0.01	<0.01	<0.01	<0.01
Cu	<0.01	⟨0.01	⟨0.01	<0.01	<0.01	⟨0.01	<0.01	<0.01	<0.01	<0.01	<0.01
Fe	41.83	2.60	28.54	44.68	6.29	28.56	12.71	8.15	8.64	16.33	37.22
K	<0.01	0.26	0.40	0.44	1.29	<0.01	1.12	1.30	1.43	1.42	0.76
Mg	0.01	0.04	0.06	0.15	0.33	0.01	0.14	0.18	0.08	0.16	0.07
Na	0.01	0.01	0.02	0.15	0.19	0.01	0.11	0.08	0.09	0.12	0.08
P	0.04	0.01	0.05	0.04	0.04	0.05	0.03	0.02	0.02	0.03	0.03
S	3.01	0.08	1.33	4.14	0.67	4.63	1.94	2.02	1.77	2.69	3.89
Ti	0.01	0.19	0.15	0.09	0.48	⟨0.01	0.32	0.38	0.23	0.30	0.12

Table 4
The chemical composition (trace elements in ppm) of CMD liberations and streams receiving CMD in the Tubarao river.

Sample	As	Ba	Be	Cd	Ce	Co	Cr	Cs	Cu	Dy	Er	Eu	Ga	Gd	Ge	Hf
DR1	5.8	3.1	<0.8	<0.8	1.9	1.0	11.8	<0.8	3.6	<0.8	<0.8	<0.8	<0.8	<0.8	<0.8	<0.8
DR2	7.2	41.4	<0.8	<0.8	19.3	1.1	10.3	1.1	6.9	<0.8	<0.8	<0.8	4.2	1.2	1.1	1.0
DR3	76.5	61.3	<0.8	<0.8	25.0	0.9	20.5	2.3	4.2	<0.8	<0.8	<0.8	7.5	1.6	1.0	11
DR4	19.0	85.5	<0.8	<0.8	15.1	1.4	8.4	1.5	6.7	<0.8	<0.8	<0.8	4.6	1.0	<0.8	<0.8
DR5	14.4	270.2	2.1	<0.8	86.5	55.0	52.0	10.6	46.9	<0.8	2.3	1.0	24.2	6.5	2.4	4.2
DR6	15.0	1.4	8.6	<0.8	7.4	<0l8	21.1	<0.8	1.4	<0.8	<0.8	<0.8	<0.8	1.7	<0.8	<0.8
DR7	15.0	227.7	1.6	<0.8	59.0	2.0	42.4	6.7	15.2	<0.8	1.3	<0.8	18.1	3.9	3.1	4.2
DR8	23.7	203.2	2.4	<0.8	73.7	6.4	42.4	14.5	16.9	<0.8	2.0	0.8	23.1	5.5	3.3	3.1
DR9	10.3	167.2	1.8	<0.8	49.7	1.6	24.9	5.9	6.1	<0.8	1.5	<0.8	12.1	4.0	3.1	2.2
DR10	44.5	258.6	3.6	<0.8	93.3	5.3	59.5	11.4	22.9	<0.8	2.6	1.0	19.0	7.3	6.9	4.6
DR11	19.3	135.7	1.0	<0.8	28.1	4.2	17.8	3.1	13.1	<0.8	<0.8	<0.8	5.2	2.2	2.7	1.3

Sample	La	Li	Lu	Mn	Mo	Nb	Nd	Ni	Pb	Pr	Rb	Sc	Se	Sm	Sn
DR1	<0.8	0.7	<0.8	67.9	<0.8	<0.8	1.3	1.0	0.9	<0.8	<0.8	1.6	6.8	<0.8	<0.8
DR2	7.8	5.7	<0.8	84.2	1.1	21.3	7.6	1.3	6.1	1.9	11.0	2.7	1.8	1.5	0.5
DR3	9.4	10.8	<0.8	16.1	1.3	17.1	10.1	3.1	11.2	2.4	19.9	4.1	2.2	1.9	1.0
DR4	7.1	6.4	<0.8	66.0	<0.8	7.9	7.1	2.5	6.2	1.8	23.5	2.0	5.6	1.4	0.4
DR5	35.8	45.0	<0.8	132.4	4.4	49.5	38.3	11.2	58.7	9.1	77.2	19.3	6.5	8.0	5.4
DR6	1.2	0.8	<0.8	25.3	16.0	<0.8	7.3	2.1	2.7	1.2	<0.8	12.6	4.2	2.4	<0.8
DR7	23.7	52.9	<0.8	68.6	2.7	34.8	23.2	4.9	20.7	5.7	54.9	8.3	4.8	4.6	2.6
DR8	30.6	61.6	<0.8	137.0	3.2	43.0	30.6	10.4	53.8	7.3	81.2	11.5	7.4	6.2	4.4
DR9	19.6	31.3	<0.8	34.3	2.6	32.0	23.0	3.6	28.5	5.5	72.3	6.3	4.9	4.7	2.3
DR10	38.0	43.4	<0.8	73.5	4.8	40.1	39.9	124	97.2	9.4	78.0	15.4	7.8	8.3	4.4
DR11	11.0	12.9	<0.8	53.6	1.9	14.6	11.6	10.1	22.3	2.8	28.5	3.8	4.0	2.5	1.1

Sample	Sr	Ta	Th	Tm	U	V	W	Y	Yb	Zn	Zr	Hg
DR1	3.5	<0.8	1.7	<0.8	<0.8	62.8	<0.8	0.8	<0.8	68.4	1.6	0.0509
DR2	9.9	2.6	3.9	<0.8	1.2	21.9	2.0	4.5	<0.8	54.9		0.0326
DR3	14.3	2.4	5.2	<0.8	1.1	72.4	2.2	5.7	<0.8	12.6	54.4	0.0034
DR4	17.9	1.2	4.2	<0.8	0.8	34.4	<0.8	4.0	<0.8	8.9	28.3	0.0174
DR5	63.8	10.4	17.0	<0.8	8.6	108.8	20.9	25.1	2.7	77.8	185.6	0.2781
DR6	4.0	1.0	20.5	<0.8	<0.8	46.3	<0.8	3.2	<0.8	4.3	3.0	0.0036
DR7	33.3	6.3	10.6	<0.8	3.1	85.7	8.7	15.1	1.5	16.4	112.2	0.0779
DR8	56.7	8.7	13.6	<0.8	3.8	81.4	10.0	24.6	2.4	52.0	125.0	0.2796
DR9	28.0	5.9	11.2	<0.8	3.9	51.3	5.6	16.8	1.9	25.0	97.2	0.1382
DR10	57.1	7.3	20.1	<0.8	<0.8	123.3	7.1	31.0	3.1	83.6	251.5	0.8534
DR11	28.5	3.0	5.8	<0.8	2.5	51.2	1.5	9.2	0.9	12.3	82.1	0.1250

cadmium. DR2 and other Fe-hydroxide phases (e.g.goethite) as spheres strongly agglomerated with common morphology to schwertmannite (Fig. 3A and Table 2); this was concluded after FE-SEM analysis. Goethite may adopt initial schwertmannite morphology and size; this has been noted by other researches as well (Schwertmann and Carlson, 2005), suggesting a 1:1 alteration of schwertmannite agglomerates into those of goethite (Schwertmann and Carlson, 2005). The sulfate-rich sand grains transported via water or wind streams were shadowed by the cementation by fine-grained material; most of them were sulfates or possibly hematite (Fig. 3B). Groundwater hematite precipitation and tabular mineral grains allowed concretion formation after diagenetic events such as area agglomeration of cements and leaching of the soluble phases to form little- to medium-sized cavity inside the rocks called vugs. On the other hand, iron oxide properties are interesting as geochemical reactivity is directly linked to different sizes of oxides.

4.2. Constituent quantities and geochemical controls

Tables 3 and 4 show the Brazilian CMD geochemical composition of evaluateds. Rich sulfide minerals are generally found at coal mining operations as a result of mine of great magnitudes of coal from the anoxic subsurface and its transference to the ecosystem (Silva and Wollenschlager, 2010a). Fe-sulfide oxidation results in HEs (e.g. zinc, cadmium, nickel, and chromium) and metalloids (e.g. selenium and arsenic) contaminant leaching, low pH conditions as previous transformations form HEs acid, and leaching, which is then transported into surface and groundwater systems.

4.2.1. Nonmetals: S > Se

Sulfur-based compounds (0.08%—4.63%) were the prominent non-metal substances present in CMD polluted sediments (Table 3). The copious quantities of sulfate salts in the outcrop (Table 3) are mainly responsible for the large sulfate concentration. Sulfide oxidation (e.g., pyrite in Fig. 2) is identified to alter with water and dissolved molecular O_2 to form sulfate and/or Fe secondary hydroxides; therefore, sulfate mineral characterizations (Table 2) are the possible products of sulfide oxidation. Coal pyrite is commonly a host for potentially toxic trace elements such as arsenic, cadmium, mercury, magnesium, selenium, and lead (Finkelman, 1994). Subsequently, pyrite oxides would be released into the CMD sediments. Selenium is a rare element found in coal from Santa Catarina (Silva et al., 2009a) that is of considerable environmental interest. Selenium values (1.8—7.8 mg/L) in CMD sediments were slightly elevated (Table 4).

4.2.2. Alkalies: K > Na > Rb > Li > Cs

Water sources around coal areas could be impacted by easily soluble alkalies as they are readily soluble elements (Silva et al., 2010b). There are alkali and alkaline earth elements at the study areas; the main alkali cations were Na (0.01% and 0.19%) and K (<0.01% and 1.43%) (Table 3). The maximum values of Li (61.6 mg/L), Rb (81.2 mg/L) and Cs (14.5 mg/L) were considerably fewer than the median values of sodium and/or potassium (Table 4).

4.2.3. Alkaline earth metals: Mg > Ca > Ba > Sr > Be

Alkaline earth elements such as Mg, Ca, Ba, and Sr can be controlled with carbonate and sulfate minerals when they are

available on the coal cleaning rejects. Alkaline earth metals are also common in rock-forming minerals and could occur in leachates as a result of acid leaching of CCR (Silva et al., 2010b). Furthermore, the hardness cations (e.g., Ca and Mg) are important in mitigating aquatic metal toxicity. In general, alkaline earth elements are very reactive and owing to that, they are not found free in nature. The predominant alkaline earth cations are calcium (<0.01% and 0.32%) and Mg (0.01% and 0.33%) (Table 3). Fig. 5 shows gypsum formation, which combines with Ca released by calcite dissolution and SO_4^{2-} from the CMD in coal abandoned area, possibly contributing to calcium distribution/precipitation in CMD. The maximum values observed for Sr, Be, and Ba were 63.8 mg/L, 8.6 mg/L, and 270.2 mg/L (Table 4).

4.2.4. Metalloid: As and Se

The main origin of CMD is the parent minerals from and amorphous phases which the coal cleaning residues are derived. The disturbance by coal mining operations possibly poses an environmental risk resulting from the As leaching (Silva et al., 2010b).

In our FE-SEM results, the As mobility is correlated primarily with a high affinity for Fe (hydr)oxides (by absorption and/or co-precipitation with the iron secondary phases), Fe sulfates (the substitution of As by Fe in iron sulfates), organic matter, and gibbsite surface; the extent of correlation depends on several biogeochemical factors.

To understand how arsenic occurrence in contaminated CMD changes as a function of area conditions, sampled sediment cores were taken from HR-TEM analysis. Because As is associated with submicron grains, it is extremely difficult to analyze using standard methods (e.g., Raman and XRD). Our observations indicated that arsenic in CMD sediments is less mobile, and, therefore, it is less bioavailable when water is kept at a constant level and the speciation of total arsenic proportions indicates that As^{3+} is more abundant than As^{5+}.

4.2.5. Transition metals: Fe > Ti > Zr > Mn > V > Zn > Cr > Cu > Mo > Ni > W > Co > Hf > Cd

Total iron concentrations in studied CMD sediments ranged between 2.60% and 44.68% (Table 3). The Fe leaching pattern differed from amorphous phases/mineral to organic rich samples and depended on whether Fe-sulfides particles were current (Silva et al., 2010c, d). Although the leaching pattern of Fe is associated with the geochemistry solubility of Fe phases (e.g., jarosite, hmetite, and goethite presented in Fig. 3A) in the samples affected by the Fe-sulfide spill, other phases control Fe solubility, and here Fe served an excellent index for the presence of Fe-sulfide particulates in the contaminated CMD samples. Fe is quickly leached and its concentration was low in the solution because most part of the total Fe was Fe^{3+}, which is very unstable in oxidant systems and at low pH values (Brookins, 1988). This group of samples presents a dissolution pH close to neutrality (<5).

Previous studies of many HEs, such as Pb, As, Ni, Cu, Zn, Cr, and Cd, have stated that they are present as dissolved uncomplex aqueous ions, and thus, they are readily bioavailable (Silva et al., 2009a). The high concentration of mobile Cd and Zn and Cd toxicity can cause environmental harm. The initial source of Cu and Zn is likely to be either sulfide minerals (e.g., sphalerite) or carbonate minerals, if they were present in the mine waste material. In addition, the increase of cadmium, Pb, and zinc in the upper layer of the core samples of CMD sediments from various rivers in the Brazilian coal zone is very high, considerably exceeding the local geochemical background. The release from secondary minerals observed by FE-SEM and HR-TEM is a likely source of these elements in CMD sediments. Our measurements also suggest that

mobile HEs can migrate into groundwater, whereas the groundwater itself can leach some chemicals from river sediments because of a relatively high water table in the study area, especially during rainfall periods. Cadmium is crucial in the CMD risk assessment because of its high mobility and toxicity. These data are important for water/sediment management in the transboundary coal zone rivers catchment situated in the Brazilian coal area.

Although there are Mn bearing phases, this HE can occur as impurities in any sulfide minerals and its release is also associated with the sludge oxidation process. In general, Mn chemically behaves similarly to Fe in nature. In oxidizing environments with evaluated acid CMD, the most stable compound is its dioxide, MnO_2. The biogeochemistry of Mn is very complex due to the following reasons: Mn in coal cleaning residues can exist in several oxidation states; the oxides of Mn can exist in several crystalline or pseudocrystalline states; the oxides can form coprecipitates with Fe oxides; and oxidation reactions involving Mn are influenced by physical, chemical, and microbiological factors. Mn concentrations in CMD sediments fluctuated between 16.1 ppm and 132.4 ppm (Table 4). The conditions of high acidity in the oxidation dissolution of these samples do not favor the precipitation of Mn that requires an alkaline pH and continuous mobilization for a long period.

Cr has numerous sources as it was distinguished by Fe-SEM/EDS dates on mineral surfaces, where it may form Fe oxyhydroxide solids that have low solubility, thus reducing its transport to groundwater. The detailed analysis of the chemical pathways in the solution revealed that both iron and sulfur species are oxidized to generate aqueous Cr(III) and Fe(III). Fe(II) was only observed in experiments where a total removal of Cr(VI) was achieved (Mullet et al., 2007). In addition, pyrite could play an important role by controlling the redox species of chromium (Mullet et al., 2007). The FE-SEM results show that Cr mobility is correlated primarily with Fe sulfates (substitution of Cr by Fe in jarosite is of common occurrence).

Cu^{2+} ion is most environmentally relevant species to aquatic systems and is generally considered the most toxic form of Cu to aquatic life. Cu concentrations ranged from 3.6 ppm to 46.9 ppm (Table 4). In CCR zones with low sulfide concentrations, Cu practically becomes absent in the CMD sediments. The justification must be the fact of the Cu concentrations resulted of disturbance in other minerals in the coal area that contain copper. However, once strong bonded organic material, the copper becomes little mobile in, the lands studied, and able to mobilize only if absorbed for clays, oxides and hydroxides of iron and/or manganese. In short, Cu solubility in sediments depends largely on pH due to hydrolysis of Cu^{2+} at pH values above 6 and to the removal of Al^{3+} and H^+ ions from exchange sites as the pH is increased in acidic zones because in soil pH also influence the degree of complexation of Cu in solid-sediments × water solution.

Cobalt and nickel are resulting from the Fe-sulfides oxidations. The distribution pattern in the evaluated sediments by FE-SEM and HR-TEM specifies solid-phase incrementation, probable by absorption and/or co-precipitation with the iron hydroxides. In divergence, the mobilized nickel is transportable and mainly unattenuated. The maximum concentration of Co in CMD sediments was recorded at DR 8 (Table 4). Cobalt follows an immobilization standard when its concentrations increase in the dissolution with increasing sulfide concentrations. In addition, the alteration of other minerals (such as those in clays) contributes to its release.

The type of Zn forms in CCR varies considerably, depending on the type and nature of CCR constituents. However, the concentrations of Zn and Cd are accredited to the mobilization of Zn-sulphide. The most common sources of Cd and Pb pollution also produce high concentration of Zn in the environment. For example, Cd, Zn, and

Pb, to some extent, coexist in sewage and smelting emissions (Caraballo et al., 2009). Although Zn was commonly detected in the FE-SEM and HR-TEM analysis of the secondary Fe oxyhydroxides (0.19–0.58 wt.% Zn in 7 samples). The CMD sediments fraction has HEs in the range of <0.8 mg/L, 8.4–59.5 mg/L, 1.8–12.4 mg/L, 0.9–97.2 mg/L, 0.8–83.3 mg/L, 0.8–10.8 mg/L, 1.6–251.5 mg/L, 0.8–4.6 mg/L, <0.8–16.0 mg/L, 21.9–123.3 mg/L and 28.9–5671.3 mg/L for Cd, Cr, Ni, Pb, Zn, W, Zr, Hf, Mo, V, and Ti, respectively. The principal source of Cd seems to be clearly the sulfide phase with the mobilization standard congruent with the release of sulfates to the dissolution; the bivalent cadmium is predominant.

The Zn mobilization follows a linear trend with the release of sulfates in all the CCR materials, but it must depend on the CCR as it is capable of liberating considerable high concentrations of Zn (Silva et al., 2009c).

4.2.6. Other HEs

The high mobility of aluminium pattern at acidic CMD pH can be elucidated by the mobility behavior of minerals and amorphous phases, such as Fe–Al-composites. Additionally, at basic CMD, other aluminumsilicate composite may disturb the geochemistry of this HE; the aluminum precipitates mobility is similar to the distribution of Fe precipitates. The total aluminum concentration in CMD sediments ranged between 0.42% and 8.82%, and Al oxyhydroxide minerals observed by FE-SEM are readily soluble efflorescent salts that can be formed on mine waste piles and can be a source or a sink for associated trace HEs such As.

Pb is a HE in coal throughout the world (Silva et al., 2009a). Although there are >200 Pb minerals, only a few are common in the coal zone, such as galena (PbS), anglesite (PbSO$_4$), and cerusite (PbCO$_3$). The pedogenic processes, climatic and topographic effects, and microbial activities may influence the distribution of Pb in the coal mining zone. The Pb concentration in CMD sediments ranges between 0.9 mg/kg and 97.2 mg/kg. Conferring to, the field of constancy of Pb^{2+} in a Pb–S–C–O–H scheme is small, predominantly when low pH (pH < 5) are mutual with oxidizing circumstances and extreme sulfate proportions in the water system. Agreed that Pb-sulfate is insoluble, its materialization and sedimentation could immobilize Pb in studied CMD. Consequently, there will be less Pb uptake by plants around the researched coal zone.

The concentration of Sn and Ga in CMD sediments range from <0.8 mg/L to 5.4 mg/L and 0.8 mg/L to 24.2 mg/L. In addition, the high proportion of Sn, Ga, Tl, Bi were substantially less than the minimum concentrations of Al (Tables 3 and 4).

4.2.7. Mercury

Hg is a persistent neurotoxic contaminant, and adverse outcomes of Hg contamination continue to prompt scientific coal zone analyses (Zhang et al., 2008; Rallo et al., 2010). Recent studies have indicated that various environmental parameters, including dissolved sulfide, are related to Hg distribution and MeHg formation in sediments (Wolfenden et al., 2005; Drott et al., 2007) and sulfides are abundant in CMD studied (Table 2). In addition, Hg in surface sediments can be transferred to the water column through diffusion, resuspension, and released by human activities. Furthermore, it can enter the aquatic food web through Hg uptake by benthos that feed at the sediment–water interface. Hg was current in moderately low proportions in Santa Catarina CMD. This research was the first to use the Hg approach to investigate the effects of local Hg sources and environmental factors in Brazil. The results provide useful information for future studies related to the transport and fate of Hg on a coal regional scale.

5. Exposure possibilities and health risks

The geochemical relationships in studied area are very difficult and are often scientific hard to observe by actual analytical procedures. However, the minerals and amorphous phases proportions examined from the sequential extraction enable an understanding of the general circulation of each amorphous phases and mineral composites phases that are formed in the reactive material and quantifies the importance of each phase on HE immobilization. Toward a more precise sediment risk assessment, we started performing mineralogical/geochemical methods to gain insight into the ecotoxicological effectiveness of the many particle-bound compounds. In addition, the treatment of heavily CMD contaminated sediments, should be considered as very important in management strategies to avoid remobilization of HEs. Therefore, a sound strategy of treating heavy metal-contaminated sediments should be developed in Brazil.

Further research on the studied CMD discharges is warranted in the forthcoming years to obtain a realistic prediction model for water quality evolution at the basin scale, which could serve as a basis for future reclamation and/or restoration plans in the Santa Catarina coal zone.

Studied CMD sediment and solid particles were traditionally classified into (in Brazil) sand, silt and clay fractions according to their sizes. Recently, with the rapid development of coal utilization, anthropogenic nano-particles are of increasing interest and concern. Detected HR-TEM images of the extracted nanoparticles indicated the particles had irregular shapes with at least one dimension less than 100 nm. Detected ultra-fine/nano-particles may be clustered and form aggregates in aqueous suspension. However, utilized ultra-sonication segregates ultra-fine/nano-particles and allows nano-particles to remain in the ultra-fine and nanoscale size distribution. Several studies have been demonstrated on the behavior and fate of nano-particles released into the environment, especially with the aim of studding their effects on the human health and ecosystems (Sharma et al., 2015).

6. Conclusions

The present work merges the records on the mineralogical and geochemical of CMD areas that were studied in 2008 in Santa Catarina, Brazil. Actually, it is very hard to calculate whether the CMD geochemistry is experiencing some kind of long temporal development. The sulfide often mineral and/or amorphous, is a less robust and could increase HEs (e.g., Cr, Co, Cu, Hg, Mn, Ni, As, and Pb). The high concentration of HEs was observed in some CMD repetitive zones, which explains the good relationship between several HEs. The results indicated that these HEs are significantly present in the nanominerals and amorphous phases. While similar to iron composites in their structure, as determinate by utilized electron beam, the ochers are discrete and present in low proportions at studied coal area. The presented data indicate that the size of the CMD sediment interfere not only the partitioning of HEs in various sediments particles size fractions. Ultrafine and nano-particles CDM sediments containing more HEs increase the potential environmental risks of coimmobilization of HEs by river colloids. Therefore, future studies must focus, in a better way, on the geochemistry of individual elements in the environments under consideration and how they change over time to predict future changes in their availability. Therefore, in a complex environment such as a coal-impacted estuary, the use of an advanced electron beam would be recommended for the complete assessment of

sediments. The dates can provide a basis for Brazilian government authority in the researched zone to manage HEs pollution.

Acknowledgements

References

Admiraal, W., Tubbing, G.M.J., Breebaart, L., 1995. Effects of phytoplankton on metal partitioning in the lower river Rhine. Water Research 29, 3941–3946.

Aleksander-Kwaterczak, U., Helios-Rybicka, E., 2009. Contaminated sediments as a potential source of Zn, Pb, and Cd for a river system in the historical metalliferous ore mining and smelting industry area of South Poland. Journal of Soils and Sediments 9, 13–22.

Allen, Y., Calow, P., Baird, D.J., 1995. A mechanistic model of contaminant induced feeding inhibition in Daphnia magna. Environmental Toxicology & Chemistry 149, 1625–1630.

Alpers, C.N., Majzlan, J., Bender, K.C., Bishop, J.L., Coleman, M.L., Dyar, M.D., McCleskey, R.B., Myneni, S.C.B., Nordstrom, D.K., Sobron, P., 2008. Chemistry and spectroscopy of iron-sulfate minerals from Iron Mountain, California, U.S.A. Geochimica et Cosmochimica Acta 72, A17.

Antunes, S.C., Pereira, R., Goncalves, F., 2007. Evaluation of the potential toxicity (acute and chronic) of sediments from abandoned uranium mine ponds. Journal of Soils and Sediments 7, 368–376.

Balachandran, K.K., Raj, C.M.L., Nair, M., Joseph, T., Sheeba, P., Venugopal, P., 2005. Heavy metal accumulation in a flow restricted, tropical estuary. Estuarine Coastal and Shelf Science 65, 361–370.

Birch, G., Taylor, S., 1999. Source of heavy metals in sediments of the Port Jackson estuary, Australia. The Science of the Total Environment 227, 123–138.

Bishop, J., Coleman, M., Sobron, P., Lane, M., Dyar, D., Schiffman, P., 2008. Sulfates on Mars: Comparison with spectral properties of analog sites. Geochimica et Cosmochimica Acta 72, A85.

Blowes, D.W., Ptacek, C.J., Jambor, J.L., Weisener, C.G., 2003. The geochemistry of acid mine drainage. In: Lollar, B.S. (Ed.), Environmental Geochemistry. In: Holland, H.D., Turekian, K.K. (Eds.), Treatise on Geochemistry, vol. 9. Elsevier–Pergamon, Oxford, pp. 149–204.

Bonny, S., Jones, B., 2003. Canadian Journal of Earth Sciences 40, 1483.

Brookins, D.G., 1988. Eh-pH Diagrams for Geochemistry. Springer-Verlang, New York, p. 75p.

Buckley, A.N., Wouterlood, H.J., Woods, R., 1989. The surface composition of natural sphalerites under oxidative leaching conditions. Hydrometallurgy 22, 39–56.

Burton Jr., G.A., 2002. Sediment quality criteria in use around the world. Limnology 3, 65–75.

Caraballo, M.A., Rötting, T.S., Nieto, J.M., Ayora, C., 2009. Sequential extraction and DXRD applicability to poorly crystalline Fe- and Al-phase characterization from an acid mine water passive remediation system. American Mineralogist 94, 1029–1038.

Chen, C.J., Jiang, W.T., 2008. An EXAFS and FTIR study on the sulfate and arsenate configurations of schwertmannite. Geochimica et Cosmochimica Acta 72, 152.

Chen, Y., Shah, N., Huggins, F.E., Huffman, G.P., 2004. Investigation of the microcharacteristics of PM2.5 in residual oil fly ash by analytical transmission electron microscopy. Environmental Science and Technology 38, 6553–6560.

Cornell, R.M., Schwertmann, U., 2003. The Iron Oxides: Structure, Properties, Reactions, Occurrence and Uses, Second, Completely Revised and Extended Ed. Wiley-VCH Verlag GmbH & Co. KGaA, Weinheim.

Dai, S., Zou, J., Jiang, Y., Ward, C.R., Wang, X., Li, T., et al., 2011a. Mineralogical and geochemical com- positions of the Pennsylvanian coal in the Adaohai Mine, Daqingshan Coalfield, Inner Mongolia, China: modes of occurrence and origin of diaspore, gorceixite, and ammonian illite. International Journal of Coal Geology 94, 250–270.

Dai, S., Wang, X., Seredin, V.V., Hower, J.C., Ward, C.R., O'Keefe, J.M.K., Li, T., Li, X., Liu, H., Xue, W., Zhao, L., 2011b. Petrology, mineralogy, and geochemistry of the Ge-rich coal from the Wulantuga Ge ore deposit, Inner Mongolia, China: new data and genetic implications. International Journal of Coal Geology 90, 72–99.

Dold, B., 2003a. Dissolution kinetics of schwertmannite and ferrihydrite in oxidized mine samples and their detection by differential X-ray diffraction (DXRD). Applied Geochemistry 18, 1531–1540.

Dold, B., 2003b. Speciation of the most soluble phases in a sequential extraction procedure adapted for geochemical studies of copper sulfide mine waste. Journal of Geochemical Exploration 80, 55–68.

Drott, A., Lambertsson, L., Björn, E., Skyllberg, U., 2007. Importance of dissolved neutral sulfides for methyl mercury production in contaminated sediments. Environmental Science & Technology 41, 2270–2276.

Eggleton, J., Thomas, K.V., 2004. A review of factors affecting the release and bioavailability of contaminants during sediment disturbance events. Environment International 30, 973–980.

España, J.S., Pamo, E.L., Santofimia, E., Aduvire, O., Reyes, J., Barettino, D., 2005. Acid mine drainage in the Iberian Pyrite Belt (Odiel river watershed, Huelva, SW Spain): Geochemistry, mineralogy and environmental implications. Applied Geochemistry 20, 1320–1356.

Finkelman, R.B., 1994. Modes of occurrence of potentially hazardous elements in coal: levels of confidence. Fuel Processing Technology 39, 21.

Fukushi, K., Sasaki, M., Sato, T., Yanese, N., Amano, H., Ikeda, H., 2003. A natural attenuation of arsenic in drainage from an abandoned arsenic mine dump. Applied Geochemistry 18, 1267–1278.

Gagliano, W.B., Brill, M.R., Bigham, J.M., Jones, F.S., Traina, S.J., 2004. Chemistry and mineralogy of ochreous sediments in a constructed mine drainage wetland. Geochimica et Cosmochimica Acta 68, 2119–2128.

Galatto, S.L., Peterson, M., Alexandre, N.Z., da Costa, J.A.D., Izidoro, G., Sorato, L., Levati, M., 2009. Incorporação de resíduo do tratamento de drenagem ácida em massa de cerâmica vermelha. Cerâmica 55, 53–60.

Giere, R., Blackford, M., Smith, K., 2006. TEM Study of PM2.5 Emitted from Coal and Tire Combustion in a Thermal Power Station. Environmental Science & Technology 40, 6235–6240.

Guedes, A., Valentim, B., Prieto, A.C., Sanz, A., Flores, D., Noronha, F., 2008. Characterization of fly ash from a power plant and surroundings by micro-Raman spectroscopy. International Journal of Coal Geology 73, 359–370.

Guillén, J., Bourrin, F., Palanques, A., Durrieu de Madron, X., Puig, P., Buscail, R., 2006. Sediment dynamics during wet and dry storm events on the Têt inner shelf (SW Gulf of Lions). Marine Geology 234, 129–142.

Hammarstrom, J.M., Seal, R.R., Meier, A.L., 2005. Secondary sulfate minerals associated with acid drainage in the eastern US: recycling of metals and acidity in surficial environments. Chemical Geology 215, 407–431.

Hammarstrom, J.M., Seal, R.R., Meier, A.L., Jackson, J.C., 2003. Weathering of sulfidic shale and copper mine waste: secondary minerals and metal cycling in Great Smoky Mountains National Park, Tennessee, and North Carolina, USA. Environmental Geology 45, 35–57.

Kumpulainen, S., Carlson, L., Raisanen, M.L., 2007. Seasonal variations of ochreous precipitates in mine effluents in Finland. Applied Geochemistry 22, 760–777.

Lattuada, R.M., Menezes, C.T.B., Pavei, P.T., Peralba, M.C.R., Dos Santos, J.H.Z., 2009. Determination of metals by total reflection X-ray fluorescence and evaluation of toxicity of a river impacted by coal mining in the south of Brazil. Journal of Hazardous Materials 163, 531–537.

Marcello, R.R., Galato, S., Peterson, M., Riella, H.G., Bernardin, A.M., 2008. Inorganic pigments made from the recycling of coal mine drainage treatment sludge. Journal of Environmental Management 88, 1280–1284.

Mullet, M., Demoisson, F., Humbert, B., Michot, L.J., Vantelon, D., 2007. Aqueous Cr(VI) reduction by pyrite: Speciation and characterisation of the solid phases by X-ray photoelectron, Raman and X-ray absorption spectroscopies. Geochimica et Cosmochimica Acta 71, 3257–3271.

Nielsen, U.G., Majzlan, J., Grey, C.P., 2008. Determination and Quantification of the Local Environments in Stoichiometric and Defects Jarosite bt Solid-State 2H NMR Spectroscopy. Chemistry of Materials 20, 2234–2241.

Peretyazhko, T., Zachara, J.M., Boily, J.-F., Xia, Y., Gassman, P.L., Arey, B.W., Burgos, W.D., 2009. Mineralogical transformations controlling acid mine drainage chemistry. Chemical Geology 262, 169–178.

Pruvot, C., Douay, F., Fourrier, H., Waterlot, C., 2006. Heavy metals in soil, crops and grass as a source of human exposure in the former mining areas. Journal of Soils and Sediments 6, 215–220.

Rallo, M., Lopez-Anton, M.A., Meij, R., Perry, R., Maroto-Valer, M.M., 2010. Study of mercury in by-products from a Dutch co-combustion power station. Journal of Hazardous Materials 174, 28–33.

Regenspurg, S., Brand, A., Peiffer, S., 2004. Formation and stability of schwertmannite in acidic mining lakes. Geochimica et Cosmochimica Acta 68, 1185–1197.

Rodriguez-Iruretagoiena, A., de Vallejuelo, S.F.O., de Diego, A., de Leão, F.B., de Medeiros, D., Oliveira, M.L.S., Tafarel, S.R., Arana, G., Madariaga, J.M., Silva, L.F.O., 2016. The mobilization of hazardous elements after a tropical storm event in a polluted estuary. The Science of the Total Environment 565, 721–729.

Root, R.A., Dixit, S., Campbell, K.M., Jew, A.D., Hering, J.G., O'Day, P.A., 2007. Arsenic sequestration by sorption processes in high-iron sediments. Geochimica et Cosmochimica Acta 71, 5782–5803.

Sharma, V.K., Filip, J., Zboril, R., Varma, R.S., 2015. Natural inorganic nanoparticles - formation, fate, and toxicity in the environment. Chemical Society Reviews 47, 8410–8423.

Schneider, I.L., Teixeira, E.C., Rodrigues, M.L.K., Rolim, S.B.A., 2014. Metal content and distribution in surface sediments in an industrial region. Annals of the Brazilian Academy of Sciences 86, 1043–1061.

Schwertmann, U., Carlson, L., 2005. The pH-dependent transformation of schwertmannite to goethite at 25 °C. Clay Minerals 40, 63–66.

Silva, L.F.O., Oliveira, M.L.S., da Boit, K.M., Finkelman, R.B., 2009a. Characterization of Santa Catarina (Brazil) coal with respect to Human Health and Environmental Concerns. Environmental Geochemistry and Health 31, 475–485.

Silva, L.F.O., Moreno, T., Querol, X., 2009b. An introductory TEM study of Fe-nanominerals within coal fly ash. The Science of the Total Environment 407, 4972–4974.

Silva, L.F.O., Finkelman, R.B., Macias, F., Oliveira, M.L.S., 2009c. Self-Assemblage of Mineral Matter in some Brazilian Coal Mining. In: Proceedings of the: International Conference on Coal Science & Technology (ICCS&T), South Africa.

Silva, L.F.O., Wollenschlager, M.A., 2010a. Preliminary study of Coal Mining Drainage and Environmental Health in the Santa Catarina region. Brazil Environmental Geochemistry and Health 33, 55–65.

Silva, L.F.O., Izquierdo, M., Querol, X., Finkelman, R.B., Towler, M., Pérez-López, R., Macias, F., 2010b. Leaching of potential hazardous elements of Coal Cleaning Residues. Environmental Monitoring and Assessment 175, 109–126.

Silva, L.F.O., Finkelman, R.B., Macias, F., Oliveira, M.L.S., 2010c. Mineral Matter in some Brazilian Coal Cleaning Residues. Environmental Monitoring and Assessment 175, 109–126.

Silva, L.F.O., Guedes, A., de Vallejuelo, S.Fdez-Ortiz, Madariaga, J.M., 2010d. Multianalytical approach to characterize the minerals associated to coals and diagnose their potential risk by using combined instrumental micro-spectroscopic techniques and thermodynamic speciation. Fuel 94, 52–63.

Stanton, M.R., Gemery-Hill, P.A., Shanks III, W.C., Taylor, C.D., 2008. Rates of zinc and trace metal release from dissolving sphalerite at pH 2.0–4.0. Applied Geochemistry 23, 136–147.

Tiede, K., Hassellöv, M., Breitbarthc, E., Chaudhryb, Q., Boxall, A.B.A., 2009. Considerations for environmental fate and ecotoxicity testing to support environmental risk assessments for engineered nanoparticles. Journal of Chromatography A 1216, 503–509.

Valente, T.M., Gomes, C.L., 2009. Occurrence, properties and pollution potential of environmental minerals in acid mine drainage. The Science of the Total Environment 407, 1135–1152.

Vaufleury, A.G., Pihan, F., 2002. Methods for toxicity assessment of contaminated soil by oral or dermal uptake in land snails: Metal bioavailability and bio-accumulation. Environmental Toxicology & Chemistry 21, 820–827.

Waychunas, G.A., 2009. Natural nanoparticle structure, properties and reactivity from X-ray studies. Powder Diffraction 24, 89–93.

Wolfenden, S., Charnock, J.M., Hilton, J., Livens, F.R., Vaughan, D.J., 2005. Sulfide species as a sink for mercury in lake sediments. Environmental Science & Technology 39, 6644–6648.

Wong, C.K.C., Cheung, R.Y.H., Wong, M.H., 1999. Toxicological assessment of coastal sediments in Hong Kong using a flagellate, Dunaliella tertiolecta. Environmental Pollution 105, 175–183.

Zhang, L., Zhuo, Y., Chen, L., Xu, X., Chen, C., 2008. Mercury emissions from six coal -fired power plants in China. Fuel Processing Technology 89, 1033–1040.

Zimmer, M.A., Lautz, L.K., 2014. Temporal and spatial response of hyporheic zone geochemistry to a storm event. Hydrological Processes 28, 2324–2337.